ELSEVIER

Contents lists available at ScienceDirect

Progress in Oceanography

journal homepage: www.elsevier.com/locate/pocean



Implications of *Pyrosoma atlanticum* range expansion on phytoplankton standing stocks in the Northern California Current



Jessica H. O'Loughlin^a, Kim S. Bernard^{a,*}, Elizabeth A. Daly^b, Samantha Zeman^b, Jennifer L. Fisher^b, Richard D. Brodeur^{a,c}, Thomas P. Hurst^d

- ^a College of Earth, Ocean, and Atmospheric Sciences, Oregon State University, Corvallis, OR 97331, USA
- b Cooperative Institute for Marine Resources Studies, Oregon State University, Hatfield Marine Science Center, Newport, OR 97365, USA
- c National Oceanic and Atmospheric Administration, Northwest Fisheries Science Center, Hatfield Marine Science Center, Newport, OR 97365, USA
- d National Oceanic and Atmospheric Administration, Alaska Fisheries Science Center, Hatfield Marine Science Center, Newport, OR 97365, USA

ARTICLE INFO

Keywords:
Pyrosome
Tunicate
Abundance
Grazing impact
Northern California Current

ABSTRACT

Coinciding with the marine heat wave in 2014 and a strong El Niño in 2016, blooms of the tropical-temperate pelagic colonial tunicate, *Pyrosoma atlanticum*, expanded into the Northern California Current (NCC). Given the high densities of *P. atlanticum* colonies observed in the NCC, and their potential for high grazing rates, we hypothesized that the species could have a substantial negative effect on the phytoplankton standing stock in the Northeastern Pacific Ocean. In the late winter, spring and early autumn of 2018, we measured abundances and length frequencies of *P. atlanticum* colonies off the coast of Oregon and estimated their spring grazing impact on the local phytoplankton standing stock. Abundances of *P. atlanticum* peaked in late winter (0.7 colonies m⁻³), dropped off in spring (0.42 colonies m⁻³), and declined to near-absent in early autumn (0.07 colonies m⁻³). We observed a doubling in the median size of *P. atlanticum* colonies from late winter to spring, followed by a decline in size in early autumn. With their high individual colony gut pigment contents and bloom densities, the overall spring grazing impact of *P. atlanticum* was substantial, reaching a maximum of 22% of the available phytoplankton standing stock.

1. Introduction

The pyrosome, Pyrosoma atlanticum, is the most widespread and common pelagic colonial tunicate in the Order Pyrosomida (class Thaliacea), and is known to have a distribution range that has historically been limited to warm, tropical-temperate waters between 50° N and 50° S (Van Soest 1981). In the California Current off the west coast of North America, P. atlanticum is primarily found south of Point Conception off Southern California (south of 34°N; Lavaniegos and Ohman 2003). However, beginning in the summer of 2014, this species was observed in low density off Southern Oregon (42°N), and in following years, the distribution range of P. atlanticum had expanded into the Northern California Current (NCC) with as yet unknown consequences (Brodeur et al., 2018; Miller et al., 2019; Sutherland et al., 2018). This warm-water species first appeared in the NCC in high densities around the occurrence of the 'warm blob' in 2014 and a strong El Niño in 2016 (Brodeur et al., 2018; Sutherland et al., 2018). In 2017, a massive bloom of P. atlanticum stretched from northern California to Alaska, with densities reaching upwards of 60,000 kg km⁻³ off the coast of

Oregon (Brodeur et al. 2018). Dense blooms of *P. atlanticum* were again observed in Oregon coastal waters from February to at least June of 2018 (Miller et al., 2019; Sutherland et al., 2018).

The colonies of *P. atlanticum* are made up of hundreds to thousands of individuals known as zooids that are oriented in a common gelatinous tunic such that the oral siphon faces the outside of the colony and the atrial siphon opens to the lumen of the colony (Madin and Deibel, 1998; Van Soest, 1981). Similar to other members of Thaliacea, *P. atlanticum* are filter feeders, using a mucous mesh to capture and consume phytoplankton (Madin and Deibel 1998). The stream of water flowing from the oral to atrial siphons is continuous and allows for both constant feeding and propulsion for extensive diel vertical migrations (Andersen and Sardou, 1994; Madin and Deibel, 1998; Perissinotto et al., 2007).

In general, tunicates exhibit extremely high clearance rates. For example, the salp, *Salpa thompsoni*, has been shown to exert a substantial impact on the phytoplankton standing stock in the Southern Ocean (Bernard et al., 2012; Loeb and Santora, 2012; Perissinotto and Pakhomov, 1998). Pyrosomes are, however, among the most

E-mail address: kim.bernard@oregonstate.edu (K.S. Bernard).

^{*} Corresponding author.

understudied planktonic consumers (Conley et al. 2018) and only two published studies have investigated the grazing impact of *P. atlanticum* the first in the equatorial East Atlantic Ocean (Drits et al. 1992) and the second in the South Indian Ocean (Perissinotto et al. 2007). In both studies, *P. atlanticum* had high clearance rates and those in the South Indian Ocean consistently favored particles > 10 μ m (Perissinotto et al. 2007). High colony densities combined with high clearance rates (\sim 5.5 L h⁻¹ for \sim 55 mm colony) were estimated to remove up to 53% of the phytoplankton standing stock per night in the equatorial East Atlantic Ocean, with the potential to exert considerable control on local phytoplankton standing stocks (Drits et al. 1992).

Given the high densities of pyrosome colonies observed in the NCC in recent years (Brodeur et al., 2019; Miller et al., 2019; Sutherland et al., 2018), it is feasible that *P. atlanticum* could have a significant negative effect on the phytoplankton standing stock in the Northeastern Pacific Ocean and, consequently, on the zooplankton grazers that also rely on phytoplankton, including euphausiids (krill) and copepods. Indeed, other tunicates have the potential, at bloom densities, to outcompete krill for phytoplankton (Atkinson et al., 2004; Bernard et al., 2012; Hereu et al., 2006; Loeb et al., 1997). Several studies linked a long-term increase in biomass of salps in the Southern California Current to a decline in total zooplankton biomass (Hereu et al., 2006; Lavaniegos and Ohman, 2003), while declines in phytoplankton in the Gulf of Alaska were observed during a large salp bloom in 2011 (Li et al. 2016).

In upwelling areas such as the NCC, where carbon flow is primarily transferred up the food chain through zooplankton such as krill and copepods, high densities of tunicates are predicted to not only affect these key zooplankton species, but also the connection between primary production and higher trophic level species (Hereu et al. 2006). Important fishery species including salmonids (Oncorhynchus spp.) and major forage species such as anchovies and smelts rely on krill and copepods, which make up the majority of their diet (Miller et al., 2010). The low concentration of lipids in pyrosomes (Perissinotto et al. 2007) suggests that they are a sub-optimal prey item for other higher trophic levels, though there have been accounts of some fishes, invertebrates, and even marine mammals consuming them in the NCC (Archer et al., 2018; Brodeur et al., 2018). If P. atlanticum becomes a dominant grazer in the NCC and is not able to provide sufficient nutrients to key predator species, the marine food web could be altered in the US Pacific Northwest.

In this paper, we measured the late-winter, spring, and early autumn densities of *P. atlanticum* colonies off the coast of Oregon during the high abundance year of 2018 and estimated their spring grazing impact on the local phytoplankton standing stock. We also measured seasonal changes in length frequencies of colonies to understand their population dynamics in this productive coastal upwelling ecosystem.

2. Methods

2.1. Field collection and hydrographic sampling

Pyrosomes were collected during three NOAA fisheries surveys on board the R/V Bell M. Shimada in late winter (February-March), spring (early May), and early autumn (September) 2018 using a Bongo net (60 cm diameter, 335 μm mesh size) towed obliquely to a maximum depth of 100 m (or just above the sea floor at shallower stations). Collection occurred at sampling stations along the coast of Oregon, spanning from 41.9 to 45.48°N and 124.40 and 128.77°W (Fig. 1).

At each station, a CTD (Sea Bird 911) profile was conducted to collect hydrographic data and seawater samples from discrete depths to be processed for chlorophyll-a (Chl-a) concentrations to estimate phytoplankton biomass following JGOFS (1994). Briefly, seawater samples were immediately filtered through 25-mm glass-fiber filters and stored at $-20\,^{\circ}$ C. Chl-a was later extracted in the laboratory for 12 h in the dark at $-20\,^{\circ}$ C using 90% acetone as the solvent. Fluorescence was

then measured with a Turner Designs $^{\text{\tiny{M}}}$ 10-AU fluorometer (Turner Designs, Sunnyvale, CA, USA). A Model II linear regression fitted to the measured Chl-a concentrations and corresponding CTD fluorescence measurements was used to convert CTD fluorescence measurements (made at 1 m depth intervals throughout the water column) into Chl-a equivalents.

2.2. Pyrosome densities and length frequencies

At stations where pyrosomes were collected, all colonies were counted and measured for total length (cm) using a measuring stick. During our surveys, catches were not large enough to necessitate subsampling. Thus, pyrosome densities (colonies m^{-3}) were calculated as total catch count divided by the volume of seawater sampled (determined using a General Oceanics 2030 flowmeter attached to the Bongo net) and multiplied by 100 such that densities are presented as colonies per hundred cubic meters (col. 100 m^{-3}). Length measurements were used to determine length frequency distributions, which were generated for each survey.

We suspect that the Bongo net, towed obliquely within the top 100 m of the water column, likely under sampled the highly patchy pyrosomes, which tend to occur in discrete layers between 25 and 45 m, based on video camera deployments (Brodeur, unpub. data). Consequently, we have corrected our Bongo-derived abundance estimates using pyrosome abundance data collected with a 12 imes 12 m demersal trawl net towed horizontally between 30 and 42 m in May of 2018 during a separate NOAA fisheries survey conducted within our study region on board the R/V Bell M. Shimada (see Brodeur et al., 2019 for details on sampling methodology). Volumes filtered by the trawl net were calculated by multiplying the distance towed by the effective mouth area of the trawl mesh that would retain the size of the pyrosome colonies present at that time of the year. Miller et al. (2019) found a mean P. atlanticum length of ~12.5 cm collected in trawls in May of 2018, similar to the ~13 cm mean length found in the Bongo tows during the same month. We ran a One-Way ANOVA on logtransformed abundance data derived from the trawl and Bongo nets to first determine whether there were significant differences in the catches. Since May abundance estimates were significantly higher for the trawl net (mean = 0.4 colonies m⁻³; SE = 0.1 colonies m⁻³) than the Bongo net (mean = 0.05 colonies m⁻³; SE = 0.01 colonies m⁻³; p = 0.016), we have used the ratio of trawl-derived to Bongo-derived abundances (8:1) to correct the latter.

2.3. Pyrosome grazing

To determine the proportion of the NCC phytoplankton standing stock removed daily by pyrosome grazing, we first estimated colony ingestion rates using the gut fluorescence technique, originally described by Conover et al. (1986) and Båmstedt et al. (2000), and adapted by Durbin and Campbell (2007). The technique only allows for estimation of ingestion of autotrophic organisms, and therefore does not provide estimates of feeding on heterotrophic prey. Applying the adapted gut fluorescence technique, ingestion rates (I, measured as μ g Chl-a per individual, or unit body mass, per hour) can be calculated using the equation $I = G \times k$; where G is instantaneous gut pigment content (μ g Chl-a per individual or unit body mass) and k is hourly gut evacuation rate (hour $^{-1}$).

We first measured the instantaneous gut pigment content (G, µg Chl-a colony $^{-1}$) of pyrosome colonies collected during the spring (May; n = 235 colonies) and autumn (September; n = 5 colonies) 2018 surveys. Additional collections of pyrosomes for gut pigment content were made in May using (i) a 0.5-m diameter vertical net (202 µm mesh size) towed vertically to a maximum depth 100 m and (ii) a 1.5 \times 0.5 m² neuston net towed at the surface for 5 min at \sim 1 m s $^{-1}$. Note that pyrosomes collected this way were not used for abundance estimates. Pyrosome colonies were quickly removed from the plankton

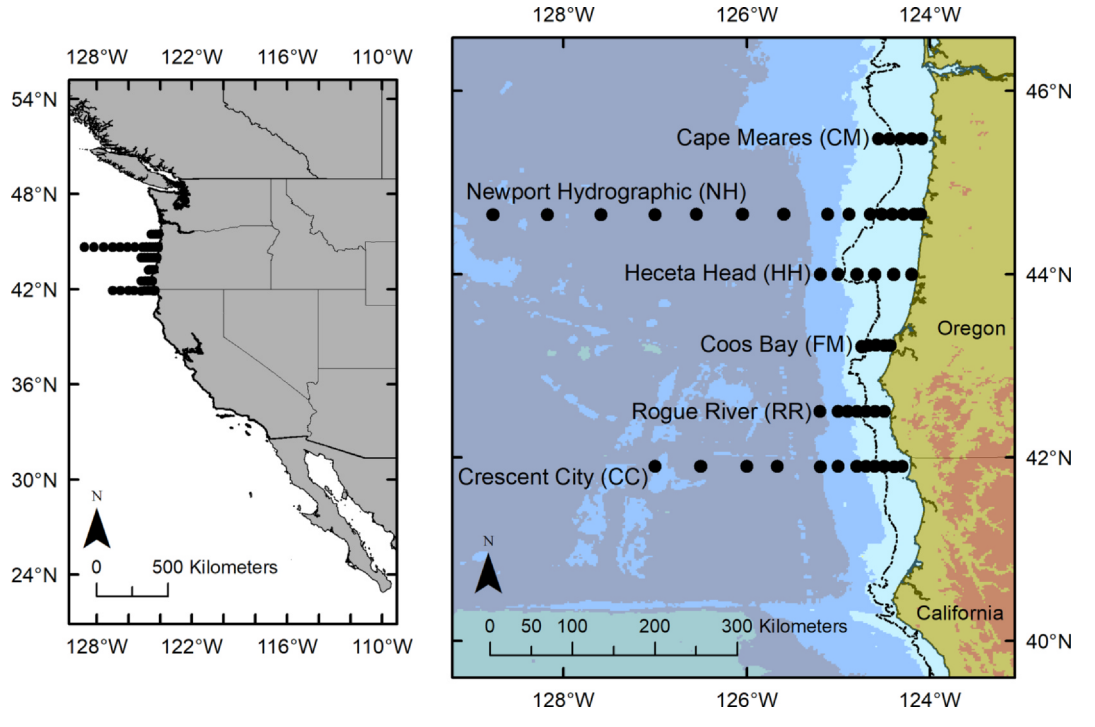


Fig. 1. Sampling station map for NOAA fisheries surveys in the Northern California Current with transect names. Dashed line is the 200 m isobath.

catch, measured for total colony length (cm) as described above, and individually frozen at -80 °C for later fluorometric analysis of gut pigment content using a calibrated Turner Designs Trilogy Fluorometer (Turner Designs, Sunnyvale, CA, USA) in the laboratory.

For pyrosomes < 10 cm in length, the whole colony was used, while for those > 10 cm in length a portion of the colony was used. In the latter case, the wet weight of the whole colony and that of the portion analyzed were recorded to extrapolate gut pigment content for the whole colony. To determine the bias associated with measuring gut pigment contents from a portion of a colony, 27 colonies (ranging in size from 7.6 to 28.5 cm) were sub-divided into 2-3 equal sections (depending on the size of the colony) and gut pigment contents were determined as both an estimate of the gut pigment content for the whole colony (calculated from each portion) as well as the actual gut pigment content of the whole colony (the sum of the gut pigment of all the portions of a given colony). The correlation between the estimated and actual gut pigment was then calculated for comparison. The ratio between estimated and actual gut pigment was close to 1:1 $(y = 0.9756x; R^2 = 0.995)$, which validated our use of sub-samples of larger colonies to estimate gut pigment. Gut pigment content, G, was then standardized by colony length (μ g Chl-a cm⁻¹). All subsequent mention of G is in standardized units.

To measure gut evacuation rate (k), two experiments were performed on freshly caught, living pyrosomes aboard the R/V Sally Ride in July 2018 from the Newport Hydrographic line. An additional experiment was also performed aboard the F/V Frosti in June 2018. However, the latter experiment and one of the two performed on the R/V Sally Ride did not show a decline in gut pigment over time, suggesting that the colonies were either no longer living or had ceased filtration of the experimental water column. As a result, these two experiments were deemed unsuccessful and have been excluded from further analysis. Individual pyrosome colonies were dip-netted from the ocean surface and placed into six 10-gallon coolers containing particle-free seawater filtered through 0.2 µm inline filter. A non-fluorescent charcoal powder was added to the filtered water to keep the pyrosomes in constant feeding conditions to aid in the digestion of previously ingested phytoplankton (Perissinotto & Pakhomov 1996). Temperature of seawater in the coolers was monitored frequently and maintained at ~ 12°C in a

refrigerated room onboard the ship. Sub-samples of 2-3 pyrosomes were removed at 10-minute intervals over a one-hour period, with the first sub-sample removed at the start of the experiment, as soon after the net was retrieved as possible (~15 min). Upon sampling, colonies were quickly measured, and subsequently frozen at -80 °C for later fluorometric analysis of gut pigment content, as described above. In order to account for natural variability in gut pigment contents of colonies, we pooled pyrosomes collected at each time point for fluorescence measurements. Further, to account for variability in colony size, gut pigment contents used in the calculation of *k* were standardized by colony length. Gut evacuation rate $(k, hour^{-1})$ was calculated as the slope of the exponential regression of standardized gut pigments over time. We note that substantial variability exists in zooplankton gut evacuation rates, dependent upon food availability and seawater temperature, among other factors (Dam and Peterson 1988). Consequently, we have only used the k value obtained here to estimate pyrosome ingestion rates for May when average SST was ~ 12 °C. In late-winter (February-March), average SST was ~ 9.5 °C, while in early autumn (September) it was ~ 13.5 °C.

Hourly ingestion rates (I, μ g Chl-a cm^{-1 h-1}, the product of G and k) for May were then converted to daily values, taking into account possible diel variability in gut pigment content of pyrosome colonies. For logistical reasons, we were not able to keep station for 24 h in order to assess diel variability in pyrosome gut pigment content. Therefore, diel variability in gut pigment content was determined from pyrosomes collected at different stations within the same latitudinal line in May. We used an N-way Analysis of Variance on log-transformed May gut pigment data to compare mean day (05:46 - 19:00) and night values (19:01-05:45) of gut pigment contents for pyrosomes collected along the CC (41.9°N), HH (44°N), and NH (44.65°N) transect lines. Only these lines were used for this analysis since the other lines did not have both day and night samples. We found no significant difference in mean gut pigment content by line (p = 0.2448). Mean daytime values of G across the three lines used in diel variability analysis were $0.16 \,\mu g$ Chl-a cm⁻¹ (\pm 0.14 SD), while mean night values were 0.18 μg Chl-a cm⁻¹ (\pm 0.15 SD). However, because other studies have shown that pyrosomes do exhibit diel feeding patterns (Perissinotto et al. 2007) we calculated daily ingestion rates (DIR, µg Chl-a cm⁻¹ day⁻¹) for May as

follows. For pyrosomes collected during the day:

$$DIR = (I \times H_d) + (I \times (\bar{I}_n/\bar{I}_d) \times H_n)$$

Where I is measured hourly ingestion rate, H_d is number of daylight hours (13.23 h), (I_n/I_d) is ratio of average nighttime I to average daytime I, and H_n is number of nighttime hours (10.77 h). For pyrosomes collected during the night, the equation was altered to:

$$DIR = (I \times H_n) + (I/(\bar{I}_n/\bar{I}_d) \times H_d)$$

Pyrosome community grazing rates (GR, μg Chl-a m⁻³ day⁻¹) were then calculated for May stations as:

$$GR = \sum_{j}^{M} DIR_{j} \times D_{j}$$

where M is the number of size categories (j, measured in 1 cm increments), DIR_j is average daily ingestion rate of colonies in size j, and D_j is the density of colonies (colonies m⁻³) of size j at that location.

The spring grazing impact (GI) was then determined as the percentage of the phytoplankton standing stock (averaged over the water column) removed daily by *P. atlanticum* at each station in May.

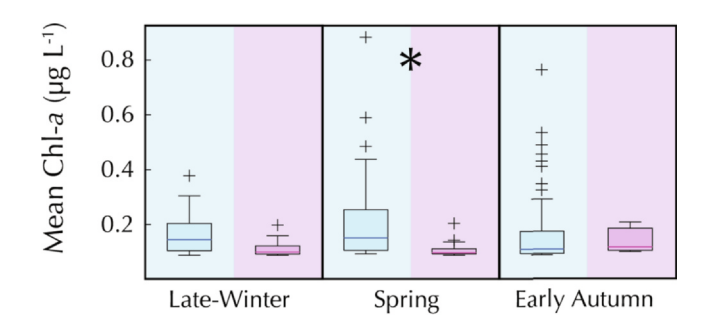
3. Results

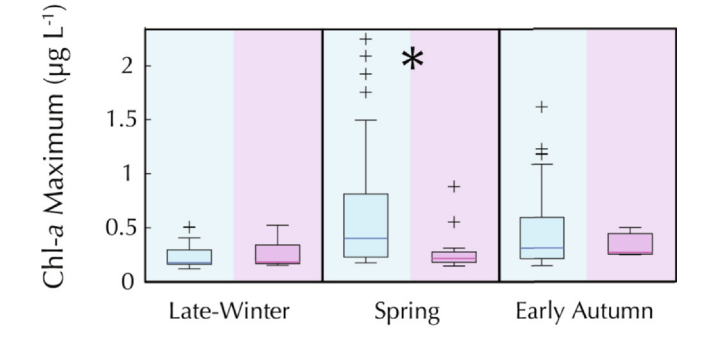
3.1. Chlorophyll-a concentrations

Average water column Chl-a concentrations ($\mu g L^{-1}$) where P. atlanticum colonies were present during the three surveys of our study varied from a median of 0.1 μ g L⁻¹ (interquartile range, IQR = 0.03 μ g L^{-1}) in late-winter (February-March), 0.1 μ g L^{-1} (IQR = 0.05 μ g L^{-1}) in spring (May), and 0.11 μ g L⁻¹ (IQR = 0.09 μ g L⁻¹) in autumn (September) (Fig. 2). In late winter and early autumn, there were no significant differences in Chl-a concentrations between stations where pyrosomes were present and where they were absent (Kruskal-Wallis test with Bonferroni adjustment; p > 0.0056; Fig. 2). However, in spring, stations without pyrosomes had significantly higher Chl-a concentrations (0.13 $\mu g L^{-1}$; IQR = 0.08 $\mu g L^{-1}$) than those with pyrosomes (Kruskal-Wallis test with Bonferroni adjustment; p < 0.001; Fig. 2). Median values for deep Chl-a maximum (DCM) were 0.18 µg L^{-1} (IQR = 0.17 µg L^{-1}), 0.19 µg L^{-1} (IQR = 0.12 µg L^{-1}), and $0.22 \mu g L^{-1}$ (IQR = $0.17 \mu g L^{-1}$) in late-winter, spring and autumn, respectively. With a similar trend to average water column Chl-a concentrations, DCM in spring was significantly higher (0.28 µg L⁻¹; IQR = $0.31 \,\mu g \, L^{-1}$) at stations without pyrosomes than at stations with pyrosomes (Kruskal-Wallis test with Bonferroni adjustment; p < 0.001; Fig. 2). Water column integrated Chl-a concentrations ranged from a median of 62 mg Chl-a m⁻² (IQR = 26.7 mg Chl-a m⁻²), 56.7 mg Chl-a m⁻² (IQR = 28 mg Chl-a m⁻²), and 48.7 mg Chl-a m⁻² (IQR = 31 mg Chl-a m⁻²) in late-winter, spring and autumn, respectively. There were no significant differences in integrated Chl-a concentrations between stations with and without pyrosomes in late-winter and early autumn, but stations without pyrosomes had significantly higher median integrated Chl-a concentrations (74 mg Chl-a m⁻²; $IQR = 32.3 \text{ mg Chl-} a \text{ m}^{-2}$) than those with pyrosomes (Kruskal-Wallis test with Bonferroni adjustment; p = 0.0048; Fig. 2).

3.2. Pyrosome densities and colony size

Pyrosoma atlanticum colonies were recorded at 17 out of 50 stations occupied in February-March, 30 out of 50 stations occupied in May, and only 3 out of 50 stations occupied in September. At stations where colonies were present, corrected densities (see Methods) were significantly greater (Tukey's HSD on log-transformed density data; p = 0.048) in the February-March survey (Mean = 0.70 col. m $^{-3}$; SE = 0.15 col. m $^{-3}$) than in the May survey (Mean = 0.42 col. m $^{-3}$; SE = 0.09 col. m $^{-3}$). May pyrosome densities were, in turn,





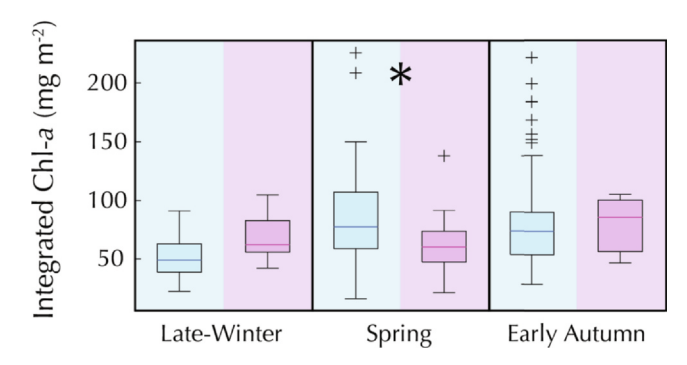


Fig. 2. Boxplots of Chlorophyll-*a* (Chl-*a*) concentrations (top panel), deep Chl-*a* maximum (DCM; middle panel) and integrated Chl-*a* concentrations (bottom panel) for late-winter (February-March), spring (May) and early autumn (September) at stations without (blue) and with (pink) pyrosomes. The asterisk denotes significant difference between median values for stations with and without pyrosomes. Kruskal-Wallis tests were performed on data since the Chl-*a*, DCM and integrated Chl-*a* data were not normally distributed.

significantly greater (Tukey's HSD on log-transformed density data; p=0.028) than those recorded in September (Mean $=0.07~{\rm col.~m}^{-3};$ SE $=0.003~{\rm col.~m}^{-3}).$ Maximum densities of P. atlanticum occurred at Newport Hydrographic Station 25 (NH25: 44.65°N; 124.65°W) during both the February-March and May surveys. Pyrosomes from the September survey were only found along the southern-most transects in our survey area: Crescent City (CC04: 41.9°N; 124.60°W; and CC05: 41.9°N; 124.70°W) and Heceta Head (HH05: 44.0°N; 125°W).

In February-March, the *P. atlanticum* community was dominated by colonies ~ 6 cm (Range 1.7-20.5 cm; SE =0.3 cm) in length (Fig. 2). By May, the dominant size of colonies had increased significantly (Tukey's HSD; p <0.001) to ~13.5 cm (Range 7-30.3 cm; SE =0.4 cm; Fig. 2). In September, pyrosome colonies were significantly smaller than either February-March (Tukey's HSD; p =0.035) or May (Tukey's HSD; p <0.001) with a dominant size of ~2.6 cm (Range 2.4-4.2 cm; SE =0.2 cm; Fig. 2).

3.3. Pyrosome grazing

The station average for gut pigment content of the colonies ranged

Table 1

Pyrosoma atlanticum densities (D, col. m⁻³) corrected for under sampling by the Bongo net and averaged by transect line for stations where colonies were present in late-winter (February-March), spring (May) and early autumn (September) of 2018. Standard error is in parenthesis and number of stations with pyrosomes (n) is provided in relation to number of stations in a transect (N). Transects lines are CM = Cape Mears; NH = Newport Hydroline; HH = Heceta Head; FM = Coos Bay; RR = Rogue River; CC = Crescent City.

Transect	Winter	Spring	Autumn
CM		0.31 (0.2) n = 2 of N = 6	n = 0 of N = 5
NH	0.87 (0.19) n = 12 of N = 15	0.65 (0.19) n = 13 of N = 16	n = 0 of N = 23
НН	0.33 (0.07) n = 3 of N = 5	0.20 (0.05) n = 5 of N = 6	0.07 $n = 1 of N = 5$
FM		0.06 $n = 1 of N = 5$	n = 0 of N = 5
RR	0.27 (0.12) n = 2 of N = 6	0.25 (0.07) n = 3 of N = 7	n = 0 of N = 7
CC	n = 0 of N = 3	0.26 (0.1) n = 6 of N = 12	0.07 (0.01) n = 2 of N = 12

Table 2 *Pyrosoma atlanticum* lengths (L, cm), gut pigment contents (G, μ g Chl-a cm⁻¹), ingestion rates (I, μ g Chl-a cm⁻¹ day⁻¹), clearance rate (F, L h⁻¹) and sample sizes (n) of colonies collected at stations (Stn.) occupied during NOAA fisheries surveys off the coast of Oregon in May and September 2018. Note that ingestion rates were not calculated for September.

Date	Stn.	Time	L	G	I	F	n
May 04	CC01	_	20.7 (2.1)	0.05 (0.02)	0.02 (0.01)	2.24	3
May 04	CC03	9:00	30.3	0.11	1.12(0)	6.41	1
May 04	CC04	17:00	25	0.06	0.65(0)	4.55	1
May 04	CC05	18:30	18.9 (2.7)	0.22 (0.01)	2.25 (1.01)	4.37	10
May 04	CC06	20:00	14.1 (1.9)	0.44 (0.32)	3.67 (2.66)	7.20	5
May 04	CC07	22:10	21	0.21	1.76(0)	5.91	1
May 05	CC10	2:57	20.5	0.17	1.44(0)	4.50	1
May 05	CC150	11:50	14.1 (3.3)	0.13 (0.03)	1.3 (0.34)	4.89	4
May 05	RR07	21:30	19.7 (4.0)	0.22 (0.05)	1.83 (0.4)	5.80	6
May 05	RR06	22:45	16.1 (3.5)	0.14 (0.10)	1.19 (0.8)	2.67	3
May 06	RR05	00:00	21.6	0.06	0.51(0)	2.99	1
May 06	FM06	20:30	20.6 (5.2)	0.24 (0.14)	1.97 (1.14)	2.33	7
May 07	HH07	2:15	15.5 (4.3)	0.15 (0.08)	1.26 (0.7)	1.70	17
May 07	HH05	4:00	12.1 (1.6)	0.11 (0.07)	0.95 (0.59)	1.29	2
May 07	HH04	5:45	17 (7.1)	0.11 (0.05)	0.94 (0.4)	0.62	10
May 07	HH03	7:00	23.3 (6.0)	0.12 (0.12	1.19 (1.22)	1.67	2
May 07	HH02	9:00	19.9 (8.0)	0.07 (0.02)	0.73 (0.22)	1.81	5
May 07	NH10	23:15	14.4 (1.5)	0.11 (0.05)	0.95 (0.39)	2.13	5
May 08	NH15	00:45	15.5 (5.7)	0.12 (0.06)	1.01 (0.48)	3.28	4
May 08	NH20	1:45	8.5	0.20	1.67(0)	5.18	1
May 08	NH25	3:30	12.9 (4.2)	0.13 (0.11)	1.1 (0.88)	4.92	40
May 08	NH35	11:30	14.9 (4.3)	0.12 (0.08)	1.28 (0.81)	4.29	25
May 08	NH45	13:30	13.1 (2.4)	0.11 (0.07)	1.42 (1.05)	3.65	4
May 08	NH65	17:00	13.1 (2.9)	0.32 (0.31)	3.29 (3.19)	3.40	5
May 08	NH85	20:00	12.4 (3.3)	0.26 (0.18)	2.2 (1.5)	3.97	17
May 08	NH105	23:00	16.0 (5.3)	0.22 (0.20)	1.84 (1.68)	3.73	16
May 09	NH125	2:00	16.0 (4.5)	0.15 (0.06)	1.24 (0.54)	3.75	11
May 09	NH150	5:15	16.1 (2.3)	0.25 (0.07)	2.07 (0.61)	5.15	10
May 09	NH175	8:30	13.3 (1.7)	0.30 (0.13)	3.05 (1.37)	1.81	6
May 09	NH200	13:30	24 (2)	0.06 (0.03)	0.62 (0.33)	1.13	3
May 10	CM25	8:30	14.6 (6.6)	0.07 (0.04)	0.71 (0.4)	2.24	3
May 10	CM20	9:45	13.7 (3.3)	0.04 (0.03)	0.37 (0.27)	6.41	6
Sept. 23	HH05	_	2.6	0.54	_	1.20	1
Sept. 25	CC04	_	3.23 (0.85)	0.06 (0.03)	_	0.14	3
Sept. 25	CC05	_	3.1	0.02	_	0.03	1

from 0.02 μ g Chl-a cm⁻¹ to 0.54 μ g Chl-a cm⁻¹ (Tables 1 and 2). Lowest average gut pigment contents were found in colonies from CC05 while highest average gut pigment contents were found in colonies from HH05. The gut evacuation experiment resulted in a k value of 0.385 h⁻¹ (95% confidence bounds: -1.041, 0.272) and a gut turnover time (1/k) of 2.6 h (Fig. 3). Daily ingestion rates (DIR) in spring

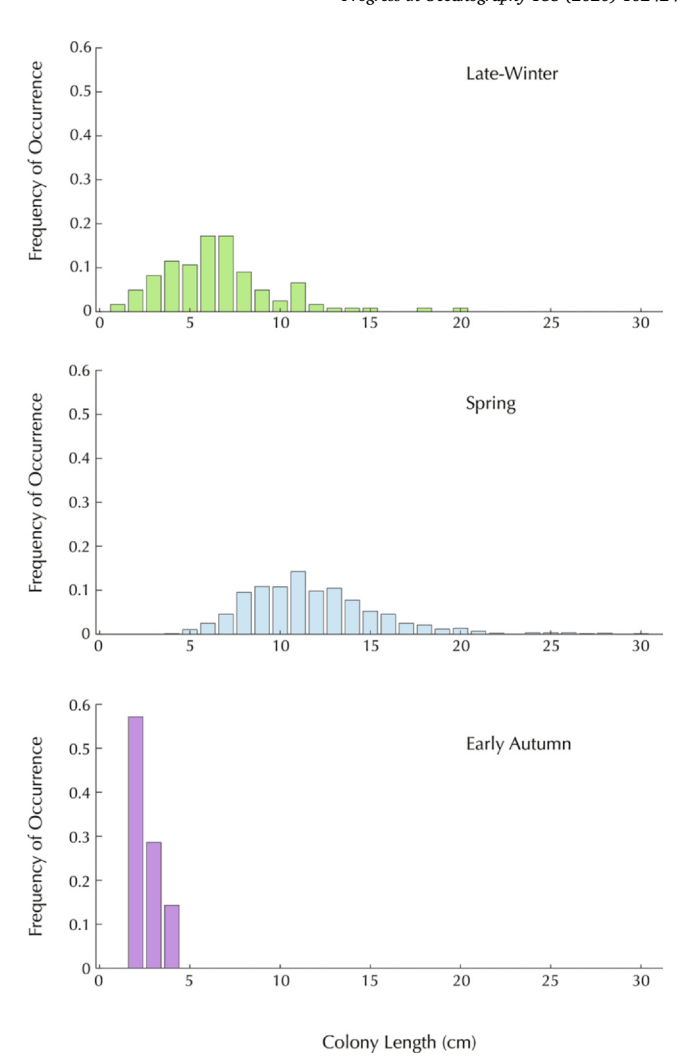


Fig. 3. *Pyrosoma atlanticum* colony length frequencies collected on NOAA fisheries surveys in late-winter (February-March), spring (May) and early autumn (September) 2018.

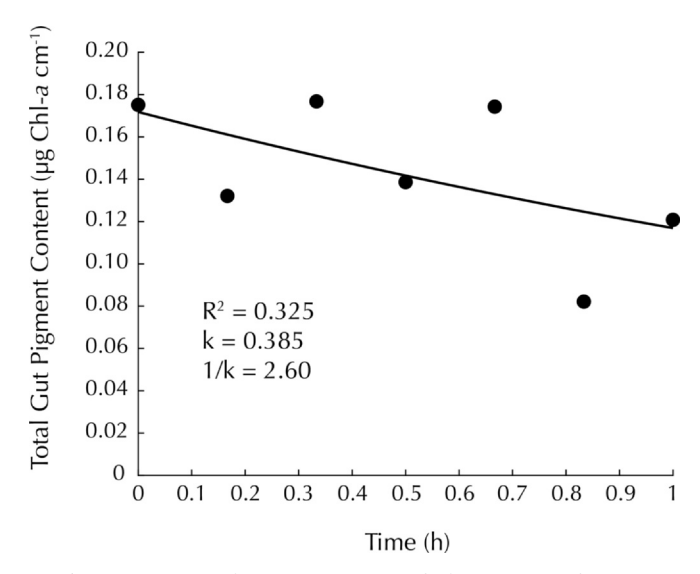


Fig. 4. Estimation of gut evacuation rate (k) for Pyrosoma atlanticum.

averaged 1.47 μ g Chl-a cm $^{-1}$ day $^{-1}$ (SE = 0.14; Table 2). Clearance rates averaged 3.58 L h $^{-1}$ (SE = 0.31 L h $^{-1}$; Table 2).Fig. 4.

Spring grazing rates (GR) for P. atlanticum in the NCC averaged

Table 3 Chlorophyll-a concentrations (SS, μ g L $^{-1}$), *Pyrosoma atlanticum* corrected densities (D, col. 100 m $^{-3}$), grazing rates (GR, μ g Chl-a m $^{-3}$), and grazing impacts (GI, %) for stations (Stn.) containing pyrosome colonies collected during a NOAA fisheries survey off the coast of Oregon in May 2018.

Date	Stn.	SS (μ g Chl a L ⁻¹)	D (col. m ⁻³)	GR (μ g Chl- a m ⁻³)	GI (%)
May 04	CC03	0.41	0.08	1.76	0.4
May 04	CC04	0.26	0.08	3.2	1.2
May 04	CC05	0.27	0.64	18.88	7.0
May 04	CC06	0.31	0.16	5.2	1.7
May 05	CC10	0.22	0.08	3.04	1.4
May 05	CC150	0.21	0.4	11.92	5.7
May 05	RR07	0.22	0.32	7.6	3.5
May 05	RR06	0.23	0.32	8.64	3.8
May 05	RR05	0.28	0.08	3.12	1.1
May 06	FM06	0.39	0.08	2	0.5
May 07	HH07	0.23	0.16	2.64	1.1
May 07	HH05	0.25	0.08	1.12	0.4
May 07	HH04	0.46	0.4	7.52	1.6
May 07	HH03	0.58	0.24	4.32	0.7
May 07	HH02	1.25	0.24	4.48	0.4
May 07	NH10	0.63	0.4	10.08	1.6
May 08	NH15	0.69	0.16	4.8	0.7
May 08	NH20	0.43	0.24	5.28	1.2
May 08	NH25	0.32	2.48	62.48	19.5
May 08	NH35	0.21	1.76	45.92	21.9
May 08	NH45	0.22	0.4	10.4	4.7
May 08	NH65	0.23	0.24	5.68	2.5
May 08	NH85	0.26	0.32	7.28	2.8
May 08	NH105	0.3	0.8	19.6	6.5
May 09	NH125	0.27	0.56	14.4	5.3
May 09	NH150	0.27	0.56	13.52	5.0
May 09	NH175	0.28	0.4	10.08	3.6
May 09	NH200	0.19	0.32	7.52	4.0
May 10	CM25	0.23	0.08	0.8	0.3
May 10	CM20	0.27	0.48	3.52	1.3

10.24 μ g Chl-a m⁻³ day⁻¹ (SE = 2.4 μ g Chl-a m⁻³ day⁻¹). Highest spring GR were observed for the southern-most line off Crescent City, and off Newport. Spring grazing impact (GI) was low throughout our study area, with pyrosomes removing an average of 3.68% (SE = 0.88%) of the available phytoplankton standing stock per day. Highest spring grazing impacts of 20 and 22% were observed off Newport at NH25 and NH35, respectively (Table 3).

4. Discussion

4.1. Range expansion by Pyrosoma atlanticum into the NCC

Pyrosoma atlanticum have undergone a recent range expansion in the California Current (Sutherland et al. 2018). As early as 2014, P. atlanticum densities increased in the NCC, and from 2015 to 2016 they moved northward from tropical-temperate waters into the NCC (Brodeur et al., 2019; Miller et al., 2019; Sutherland et al., 2018). Range expansion of this pyrosome species is thought to have been enabled by the marine heatwave event referred to as the 'warm blog', an abnormally warm stable water mass that occurred in the NE Pacific for several years starting in 2014 (Di Lorenzo & Mantua, 2016), followed by a strong El Niño in 2016 (Brodeur et al., 2019). It is possible that during this time P. atlanticum encountered favorable environmental conditions, including warmer temperatures and increased food supply, needed for their growth and development.

We observed high densities of *P. atlanticum* off the Oregon Coast during late-winter and spring of 2018. However, abundances dropped off to near-absent towards the early autumn of 2018. Our analysis of pyrosome length frequencies revealed that a doubling in average colony length occurred between collections in late-winter and spring. Age determination of gelatinous zooplankton is difficult (Gordon et al. 2004). Generally, for invertebrate species that undergo continuous

growth, age is estimated by body size (Choe and Deibel 2009). Age determination of P. atlanticum is conducted in a similar manner, with length inferring the age of a colony (longer colonies being older than shorter colonies) (Andersen and Sardou 1994). Though body size may not always be a precise method of age determination due to shrinking in response to poor environmental conditions (Choe and Deibel, 2009; Deason and Smayda, 1982; Hamner, 1974; Kremer, 1976), the doubling of average colony length recorded in our study suggests that P. atlanticum in the NCC were able to grow rapidly over a period of 1-2 months between late-winter and spring of 2018. Our results suggest that during this time P. atlanticum may have found a suitable habitat in which they could grow. Interestingly, the average length of *P. atlanticum* decreased from ~ 13 cm in spring to ~ 3 cm in early autumn. This could indicate that, towards the end of summer, P. atlanticum colonies were either (i) producing new colonies, with the older (larger) colonies dying off, or (ii) shrinking and dying off, due to unfavorable environmental conditions (Choe and Deibel, 2009; Deason and Smayda, 1982; Hamner, 1974; Kremer, 1976).

4.2. Gut evacuation rates, diel variability, and ingestion rates

Tunicates play a major role as grazers throughout the world's oceans (Conley et al., 2018; Drits et al., 1992; Madin and Deibel, 1998; Zeldis et al., 1995). As mucous-mesh feeders, tunicates can achieve consumerprey size ratios of over 10,000:1, enabling them to shorten the trophic chain and allowing more efficient energy transfer between trophic levels (Boero et al., 2008; Conley et al., 2018; Henschke et al., 2016). In addition, tunicates are known to exhibit extremely high grazing rates and species like the salp, Salpa thompsonii, have been identified as among the most important large filter feeders in terms of their filtration by wet mass (Andersen, 1998; Atkinson et al., 2004; Perissinotto et al., 1997). Salps have the capacity to remove anywhere between 10 to over 100% of the daily primary production in a given region and, at high densities, could control the phytoplankton standing stock, thereby affecting other zooplankton grazers via competition for food resources (Bernard et al., 2012; Dubischar and Bathmann, 1997; Perissinotto and Pakhomov, 1998). While there has been less research on pyrosomes, pyrosome species also exhibit high grazing rates, and species such as Pyrostremma spinosum have been shown to remove up to 17.5% of the phytoplankton standing stock in the Eastern Tropical Pacific (Décima et al. 2018). Studies conducted on P. atlanticum indicate that, during colony blooms, up to 53% of the phytoplankton standing stock could be removed in 10 h (Drits et al. 1992).

We measured grazing rates of *P. atlanticum* in the NCC using their gut fluorescence at capture. Our estimates of gut pigment content for *P. atlanticum*, obtained from colonies sampled in spring (May) of 2018, fell within the range of those reported in the literature, though our maximum values were substantially higher than previous observations (Drits et al., 1992; Perissinotto et al., 2007). Drits et al. (1992) found gut pigment contents of 2.6 to 3.9 μ g Chl-a col⁻¹ for small colonies of 5–6 cm in length. By comparison, our gut pigment values for similarly sized colonies ranged from 0.5 to 5.2 μ g Chl-a col⁻¹. For 11 to 20 cm colonies, Perissinotto et al. (2007) reported gut pigment values between 0.8 and 1.6 μ g Chl-a col⁻¹, while our measured gut pigment values for similarly sized colonies were between 0.2 and 9.2 μ g Chl-a col⁻¹.

The gut evacuation rate we obtained during our study yielded a k value of 0.385 h $^{-1}$ and a gut turnover time (1/k) of 2.6 h. Only one previous study has estimated the gut evacuation rate of P. atlanticum, and reported a k value of 0.699 h $^{-1}$ (Perissinotto et al. 2007). While seawater temperature for the Perissinotto et al. (2007) gut evacuation rate experiment was not provided in their manuscript, other experiments conducted during their study were at temperatures ranging between 13.7 and 17.8 °C. Our gut evacuation rate experiment was conducted at 12 °C, so it is possible that the difference between our values and that of Perissinotto et al. (2007) was driven by differences in temperature. Warmer seawater temperatures would increase metabolic

processes and thus gut evacuation rate (Dam and Peterson 1988). Since seawater temperatures during our spring (May) survey averaged 12 °C, our measured k value is appropriate for calculating ingestion rate of pyrosomes collected in that survey. As no gut evacuation rate experiments were performed in early autumn (September) and average SST was higher (\sim 13.5 °C) than that used in our gut evacuation rate experiments, we did not calculate ingestion rates for the few pyrosomes collected on that survey.

Whole-colony ingestion rates, averaged by station, in May were highly variable ranging between 0.1 μg Chl-a cm⁻¹ day⁻¹ (equivalent to $\sim 7.33~\mu g$ Chl-a col. $^{-1}$ day $^{-1}$) and 0.17 μg Chl-a cm $^{-1}$ day $^{-1}$ (equivalent to $\sim 40 \,\mu g \, \text{Chl-} a \, \text{col.}^{-1} \, \text{day}^{-1}$), with an average of 0.06 $\,\mu g$ Chl-a cm⁻¹ day⁻¹ (equivalent to $\sim 20 \mu g$ Chl-a col.⁻¹ day⁻¹). These values are within the low end of the range of those reported for P. atlanticum in the Indian Ocean (15.15 – 69.91 μ g Chl-a col.⁻¹ day⁻¹) (Perissinotto et al. 2007), and are substantially lower than that reported for the Atlantic Ocean (98.4 μ g Chl-a col. ⁻¹ day ⁻¹) (Drits et al. 1992). Given corresponding phytoplankton standing stocks, our observed ingestion rates equate to filtration rates of 0.6 to 7.2 L colony⁻¹h⁻¹, with an average of 3.6 L colony⁻¹h⁻¹. Our upper range is comparable to filtration rates reported for P. atlanticum in the Atlantic Ocean, 5.5 L colony⁻¹h⁻¹ (Drits et al. 1992) and on the low range of those reported for P. atlanticum in the Indian Ocean where values ranged from 3.8 to 14.4 L colony $^{-1}h^{-1}$ (Perissinotto et al. 2007).

4.3. Grazing rates and grazing impact

Pyrosomes have been shown to play an important role in pelagic ecosystems through their ability to form dense blooms and their high grazing rates (Décima et al., 2018; Drits et al., 1992; Perissinotto et al., 2007). In our study, P. atlanticum grazing rates averaged 10.24 µg Chl-a $m^{-3} d^{-1}$, with a maximum value of 62.48 µg Chl-a $m^{-3} d^{-1}$, corresponding to grazing impacts of 4% of available phytoplankton standing stock on average and 22% maximum. This is higher than grazing impacts reported for the Indian Sector of the Southern Ocean where values were typically < 1%, with the exception of one station where pyrosome grazing impact averaged 5% (Perissinotto et al. 2007). In other oceans where pyrosomes have been recorded in dense blooms, grazing impacts have been similarly high to those that we observed. For instance, at a single station in the Atlantic Ocean where pyrosomes were at bloom densities (e.g. 9.5 col. m⁻³ concentrated in the top 10 m of the water column), daily grazing impact was estimated to be 53% of available phytoplankton biomass in 10 h (Drits et al. 1992). In the Eastern Tropical Pacific, Pyrostremma spinosum communities were capable of removing as much as 17.5% of the phytoplankton standing stock daily (Décima et al. 2018).

Our results indicate that, at bloom densities, it is possible for pyrosomes to exert considerable control on phytoplankton standing stocks. Indeed, during our spring survey (May 2018), Chl-a concentrations, deep Chl-a maximum (DCM) and integrated Chl-a concentrations were significantly higher at stations where pyrosomes were absent than where they were present. While P. atlanticum could have been avoiding areas of elevated phytoplankton biomass, we suggest a more plausible reason is that grazing rates of the pyrosome colonies were sufficient to control phytoplankton standing stock at stations where they were present. This could have significant implications for key crustacean zooplankton grazers.

4.4. Implications

Rising temperature, an effect closely associated with climate change, has paved the way for range expansion of both terrestrial and marine species (Hoegh-Guldberg and Bruno, 2010; Parmesan, 2006). Temperature increases may facilitate range expansion in marine taxa through the alteration of ocean circulation patterns (Meehl et al. 2007) and the timing/duration of seasonal events, such as phytoplankton

blooms (Edwards and Richardson 2004) and coastal upwelling (Bograd et al. 2009). From phytoplankton (Neukermans et al. 2018) and reef corals (Yamano et al. 2011) to macroinvertebrates and fish (Johnson et al., 2011; Perry et al., 2005; Stewart et al., 2012), a multitude of marine species have experienced changes in their distribution range as a result of long-term warming (Pinsky et al. 2013). Indeed, numerous examples of both invertebrate and vertebrate taxa exhibiting substantial northward distribution shifts and range extensions have been documented for this recent North Pacific marine heatwave (Cavole et al., 2016; Sanford et al., 2019). Species that have successfully established themselves in previously unavailable habitats, such as the invasive lionfishes, Pterois volitans and P. miles, have had detrimental impacts on native marine ecosystems and are a threat to biodiversity in these regions (Grieve et al., 2016; Sorte et al., 2010). Poleward range expansions in all oceanic regions have been observed with an average rate of 72 ± 13 km per decade (Poloczanska et al., 2013, 2016). Ocean warming is expected to progress as greenhouse gas emissions from anthropogenic activity continues, enabling exacerbated range expansion and causing concern for the health of marine ecosystems throughout the world's oceans (Grieve et al. 2016).

Jellyfish, a loose term encompassing schyphozoans, ctenophores, and chordates (i.e. salps, pyrosomes, and appendicularians), have experienced population increases in coastal ecosystems over the past several decades (Brotz et al., 2012; Condon et al., 2013). Pelagic organisms are experiencing range expansion at a much faster rate than the global average, with invertebrate zooplankton expanding at a rate of 142 ± 28 km per decade (Poloczanska et al., 2013, 2016). More specifically, tunicates appear to be undergoing range expansions throughout all oceanic regions. In the California Current, changes in the biomass of pelagic tunicates have been linked to the decline of total zooplankton biomass (Lavaniegos and Ohman 2003). Through their short generation times and rapid growth rates, pelagic tunicates can experience massive population increases in response to favorable environmental conditions, including changes induced by anomalous events like El Niño Southern Oscillation (ENSO) cycles (Andersen, 1998; Atkinson et al., 2014; Hereu et al., 2006; Lavaniegos and Ohman,

The ability of tunicates to form blooms in response to changes in the environment can prove detrimental to other zooplankton species and may affect food web dynamics (Andersen, 1998; Dubischar et al., 2006; Lavaniegos and Ohman, 2003; Ross et al., 2014). Salpa thompsonii, a salp species inhabiting the region between the Subtropical Convergence and the Antarctic sea ice edge have moved to more southern regions in increasing frequency (Kawamura, 1986, 1987). Dense blooms of S. thompsonii have been observed at abundances upwards of 650 ind. m⁻² in the Southern Ocean while the krill species Euphausia superba has experienced a concomitant decline (Atkinson et al., 2004; Bernard et al., 2012). If temperatures continue to increase, S. thompsonii and other tunicate species could pose a serious threat to krill and other zooplankton grazers (Bernard et al. 2012). For instance, abundance of krill, especially the nearshore dominant species Thysanoessa spinifera, declined dramatically off Oregon following the arrival on the shelf of the recent marine heatwave, concurrent with the substantial increase in pyrosomes (Brodeur et al., 2019; Peterson et al., 2017). Should pelagic tunicates outcompete key crustacean grazers such as krill and copepods for phytoplankton, it is unclear how this would affect higher trophic levels that rely krill and copepods as a primary food source. Also, since pelagic tunicates are non-selective filter-feeders it is possible that, at bloom densities, their high ingestion rates could account for reduced biomass of smaller zooplankton taxa through direct predation. However, according to a recent study in the Eastern Tropical Pacific that used stable isotope analysis to infer trophic position, the pyrosome Pyrostremma spinosum is purely herbivorous (Décima et al. 2018). We were not able to assess the degree of carnivory in P. atlanticum during the present study.

5. Conclusions

Warming of the Northern California Current (NCC) off the coast of Oregon has resulted in episodic range expansion by the pyrosome, *Pyrosoma atlanticum*. Range expansion of exotic species has the potential to affect entire ecosystems and may be detrimental to ecosystem functioning. The purpose of this study was to determine the grazing impact of *P. atlanticum* on the phytoplankton standing stock of the NCC, specifically off the coast of Oregon. We found that even at the tail-end of the multi-year pyrosome "explosion" off the Oregon Coast, the grazing impact of colonies of *P. atlanticum* on the phytoplankton standing stock of the NCC was substantial, reaching 22% of the total available phytoplankton.

Declaration of Competing Interest

The authors declare that they have no known competing financial interests or personal relationships that could have appeared to influence the work reported in this paper.

Acknowledgements

We would like to thank the crew of the *R/V* Bell M. Shimada and *R/V* Elakha whose hard work was vital to this research. Special thanks also go to Kym Jacobson (Northwest Fisheries Science Center), Charles Leal (student at Oregon State University supported by the Marine Studies Initiative), and other students, technicians, and scientists who aided in data collection. Funding for this study was provided by the National Science Foundation (Grant Number 1838492).

References

- Andersen, V., 1998. Salp and pyrosomid blooms and their importance in biogeochemical cycles, p. 125-138. In: Bone, Q. (Ed.), The Biology of Pelagic Tunicates. Oxford University Press.
- Andersen, V., Sardou, J., 1994. Pyrosoma atlanticum (Tunicata, Thaliacea): Diel migration and vertical distribution as a function of colony size. J. Plankton Res. 16, 337–349
- Archer, S.K., et al., 2018. Pyrosome consumption by benthic organisms during blooms in the northeast Pacific and Gulf of Mexico. Ecology 99, 981–984.
- Atkinson, A., et al., 2014. Sardine cycles, krill declines, and locust plagues: revisiting 'wasp-waist' food webs. Trends Ecol. Evol. 29, 309–316.
- Atkinson, A., Siegel, V., Pakhomov, E., Rothery, P., 2004. Long-term decline in krill stock and increase in salps within the Southern Ocean. Nature 432, 100–103.
- Båmstedt, U., Gifford, D.J., Irigoien, X., Atkinson, A., Roman, M., 2000. Feeding. In: Harris, R.P., Wiebe, P.H., Lenz, J., Skjodal, H.R., Huntley, M. (Eds.), ICES Zooplankton Methodology Manual. Academic Press, pp. 297–399.
- Bernard, K.S., Steinberg, D.K., Schofield, O.M.E., 2012. Summertime grazing impact of the dominant macrozooplankton off the Western Antarctic Peninsula. Deep-Sea Res. I 62. 111–122.
- Boero, F., et al., 2008. Gelatinous plankton: irregularities rule the world (sometimes). Mar. Ecol. Prog. Ser. 356, 299–310.
- Bograd, S.J., Schroeder, I., Sarkar, N., Qiu, X., Sydeman, W.J., Schwing, F.B., 2009. Phenology of coastal upwelling in the California Current. Geophys. Res. Lett. 36.
- Brodeur, R., et al., 2018. An unusual gelatinous plankton event in the NE Pacific: The Great Pyrosome Bloom of 2017. PICES Press 26, 22–27.

 Predeur, R., et al., 2018. An unusual gelatinous plankton event in the NE Pacific The Company of the Comp
- Brodeur, R.D., Auth, T.D., Phillips, A.J., 2019. Major shifts in pelagic micronekton and macrozooplankton community structure in an upwelling ecosystem related to an unprecedented marine heatwave. Front. Mar. Sci. 6, 212.
- Brotz, L., Cheung, W.W.L., Kleisner, K., Pakhomov, E., Pauly, D., 2012. Increasing jellyfish populations: trends in Large Marine Ecosystems. Hydrobiologia 690, 3–20.
- Cavole, L.M., et al., 2016. Biological impacts of the 2013–2015 warm-water anomaly in the Northeast Pacific: Winners, losers, and the future. Oceanography 29, 273–285.
- Choe, N., Deibel, D., 2009. Statolith diameter as an age indicator in the planktonic tunicate Oikopleura vanhoeffeni: Variability in age-specific growth patterns in Conception Bay, Newfoundland. J. Exp. Mar. Biol. Ecol. 375, 89–98.
- Condon, R.H., et al., 2013. Recurrent jellyfish blooms are a consequence of global oscillations. Proc. Natl. Acad. Sci. 110, 1000–1005.
- Conley, K.R., Lombard, F., Sutherland, K.R., 2018. Mammoth grazers on the ocean's minuteness: a review of selective feeding using mucous meshes. Proc. Royal Soc. B: Biolog. Sci., 285.
- Conover, R.J., Durvasula, R., Roy, S., Wang, R., 1986. Probable loss of chlorophyll-derived pigments during passage through the gut of zooplankton, and some of the consequences. Limnol. Oceanogr. 31, 878–886.
- Dam, H.G., Peterson, W.T., 1988. The effect of temperature on the gut clearance rate

- constant of planktonic copepods. J. Exp. Mar. Biol. Ecol. 123, 1-14.
- Deason, E.E., Smayda, T., 1982. Experimental Evaluation of Herbivory in the Ctenophore Mnemiopsis leidyi Relevant to Ctenophore-Zooplankton-Phytoplankton Interactions in Narragansett Bay, Rhode Island, USA. J. Plankton Res. 4, 219–236.
- Décima, M., Stukel, M.R., López-López, L., Landry, M.R., 2018. The unique ecological role of pyrosomes in the Eastern Tropical Pacific. Limnol. Oceanogr. 64, 728–743.
- Drits, A.V., Arashkevich, E.G., Semenova, T.N., 1992. Pyrosoma atlanticum (Tunicate, Thaliacea): grazing impact on phytoplankton standing stock and role in organic carbon flux. J. Plankton Res. 14, 799–809.
- Dubischar, C.D., Bathmann, U.V., 1997. Grazing impact of copepods and salps on phytoplankton in the Atlantic sector of the Southern Ocean. Deep-Sea Res. II 44, 415–433.
- Dubischar, C.D., Pakhomov, E.A., Bathmann, U.V., 2006. The tunicate Salpa thompsoni ecology in the Southern Ocean II. Proximate and elemental composition. Marine Biol. 140, 625-632
- Durbin, E.G., Campbell, R.G., 2007. Reassessment of the gut pigment method for estimating in situ zooplankton ingestion. Mar. Ecol. Prog. Ser. 331, 305–307.
- Edwards, M., Richardson, A., 2004. Impact of climate change on marine pelagic phenology and trophic mismatch. Nature 430, 881.
- Gordon, M., Hatcher, C., Seymour, J., 2004. Growth and age determination of the tropical Australian cubozoan Chiropsalmus sp. Hydrobiologia 530, 339–345.
- Grieve, B., Grieve, B., Curchitser, E., Rykaczewski, R., 2016. Range expansion of the invasive lionfish in the Northwest Atlantic with climate change. Mar. Ecol. Prog. Ser. 546, 225–237
- Hamner, W.M., 1974. Growth, degrowth, and irreversible cell differentiation in Aurelia aurita. Am. Zool. 14, 833–849.
- Henschke, N., Everett, J.D., Richardson, A.J., Suthers, I.M., 2016. Rethinking the role of salps in the ocean. Trends Ecol. Evol. 31, 720–733.
- Hereu, C.M., Lavaniegos, B., Gaxiola-Castro, G., Ohman, M.D., 2006. Composition and potential grazing impact of salp assemblages off Baja California during the 1997–1999 El Niño and La Niña. Mar. Ecol. Prog. Ser. 318, 123–140.
- Hoegh-Guldberg, O., Bruno, J., 2010. The impact of climate change on the world's marine ecosystems. Science 328, 1523–1528.
- JGOFS. 1994. JGOFS Protocols, p. 210. Scientific Committee on Oceanic Research; International Council of Scientific Unions.
- Johnson, C.R., et al., 2011. Climate change cascades: Shifts in oceanography, species' ranges and subtidal marine community dynamics in eastern Tasmania. J. Exp. Mar. Biol. Feol. 400, 17–32.
- Kawamura, A., 1986. Has marine Antarctic ecosystem changed?-A tentative comparison of present and past macrozooplankton abundances. Memoirs Natl. Inst. Polar Res. 40, 197–211.
- Kawamura, A., 1987. Two series of macrozooplankton catches with the N70V net in the Indian Sector of the Antarctic Ocean. Proc. NIPR Symp. Polar Biol. 1, 84–89.
- Kremer, P., 1976. Population dynamics and ecological energetics of a pulsed zooplankton predator, the ctenophore Mnemiopsis leidyi. In: Wiley, M.L. (Ed.), Estuarine Processes. Uses, Stresses and Adaptation to the Estuary. Academic Press, pp. 197-215.
- Lavaniegos, B.E., Ohman, M.D., 2003. Long-term changes in pelagic tunicates of the California Current. Deep Sea Res. Part II 50, 2473–2498.
- Li, K., Doubleday, A.J., Galbraith, M.A., Hopcroft, R.R., 2016. High abundance of salps in the coastal Gulf of Alaska during 2011: A first record of bloom occurrence for the northern Gulf. Deep Sea Res. Part II 132, 136–145.
- Loeb, V., et al., 1997. Effects of sea-ice extent and krill or salp dominance on the Antarctic food web. Nature 387, 897–900.
- Loeb, V.J., Santora, J.A., 2012. Population dynamics of Salpa thompsoni near the Antarctic Peninsula: Growth rates and interannual variations in reproductive activity (1993–2009). Prog. Oceanogr. 96, 93–107.
- Madin, L.P., Deibel, D., 1998. Feeding and energetics of Thaliacea. In: Bone, Q. (Ed.), The Biology of Pelagic Tunicates. Oxford University Press, pp. 81–103.
- Meehl, G.A., et al., 2007. Global climate projection. In: S. Solomon et al. (Eds.), Climate Change 2007: The Physical Science Basis. Contribution of Working Group I to the Fourth Assessment Report of the Intergovernmental Panel on Climate Change. Cambridge University Press, pp. 747–845.
- Miller, R.R., et al., 2019. Distribution of pelagic thaliaceans, Thetys vagina and Pyrosoma atlanticum, during a period of mass occurrence within the California Current, pp. 94–108. CalCOFI Report.
- Miller, T.W., Brodeur, R.D., Rau, G.H., Omori, K., 2010. Prey dominance shapes trophic structure of the northern California Current pelagic food web: evidence from stable isotopes and diet analysis. Mar. Ecol. Prog. Ser. 420, 15–26.
- Neukermans, G., Oziel, L., Babin, M., 2018. Increased intrusion of warming Atlantic water leads to rapid expansion of temperate phytoplankton in the Arctic. Glob. Change Biol. 24, 2545–2553.
- Parmesan, C., 2006. Ecological and evolutionary responses to recent climate change. Annu. Rev. Ecol. Evol. Syst. 37, 637–669.
- Perissinotto, R., Mayzaud, P., Nichols, P.D., Labat, J.P., 2007. Grazing by Pyrosoma atlanticum (Tunicata, Thaliacea) in the south Indian Ocean. Mar. Ecol. Prog. Ser. 330, 1-11
- Perissinotto, R., Pakhomov, E.A., 1998. The trophic role of the tuniate Salpa thompsoni in the Antarctic marine ecosystem. J. Mar. Syst. 17, 361–374.
- Perissinotto, R., Pakhomov, E.A., McQuaid, C.D., Froneman, P.W., 1997. In situ grazing rates and daily ration of Antarctic krill Euphausia superba feeding on phytoplankton at the Antarctic Polar Front and the Marginal Ice Zone. Mar. Ecol. Prog. Ser. 160, 77, 91
- Perry, A.L., Low, P.J., Ellis, J.R., Reynolds, J.D., 2005. Climate change and distribution shifts in marine fishes. Science 308, 1912–1914.
- Peterson, W.T., et al., 2017. The pelagic ecosystem in the Northern California Current off Oregon during the 2014–2016 warm anomalies within the context of the past 20

- years. J. Geophys. Res. Oceans 122, 7267-7290.
- Pinsky, M.L., Worm, B., Fogarty, M.J., Sarmiento, J.L., Levin, S.A., 2013. Marine taxa track local climate velocities. Science 341, 1239–1242.
- Poloczanska, E.S., et al., 2013. Global imprint of climate change on marine life. Nat. Clim. Change $3,\,919$.
- Poloczanska, E.S., et al., 2016. Responses of marine organisms to climate change across oceans. Front. Mar. Sci. 3, 62.
- Ross, R.M., et al., 2014. Trends, cycles, interannual variability for three pelagic species west of the Antarctic Peninsula 1993–2008. Mar. Ecol. Prog. Ser. 515, 11–32.
- Sanford, E., Sones, J.L., García-Reyes, M., Goddard, J.H.R., Largier, J.L., 2019. Widespread shifts in the coastal biota of northern California during the 2014–2016 marine heatwaves. Nat. Sci. Rep. 9, 1–14.
- Sorte, C.J.B., Williams, S.L., Zerebecki, R.A., 2010. Ocean warming increases threat of invasive species in a marine fouling community. Ecology 91, 2198–2204.
- Stewart, J., Hazen, E., Foley, D.G., Bograd, S.J., Gilly, W., 2012. Marine predator migration during range expansion: Humboldt squid Dosidicus gigas in the northern California Current System. Mar. Ecol. Prog. Ser. 471, 135–150.
- Sutherland, K.R., Sorensen, H.L., Blondheim, O.N., Brodeur, R.D., Galloway, A.W.E., 2018. Range expansion of tropical pyrosomes in the northeast Pacific Ocean. Ecology 99, 2397–2399.
- Van Soest, R.W.M., 1981. A monograph of the Order Pyrosomatida (Tunicata, Thaliacea). J. Plankton Res. 3, 603–631.
- Yamano, H., Sugihara, K., Nomura, K., 2011. Rapid poleward range expansion of tropical reef corals in response to rising sea surface temperatures. Geophys. Res. Lett. 38, L04601.
- Zeldis, J.R., Davis, C.S., James, M.R., Ballara, S.L., Booth, W.E., Chang, F.H., 1995. Salp grazing: Effects on phytoplankton abundance, vertical distribution and taxonomic composition in a coastal habitat. Mar. Ecol. Prog. Ser. 126, 267–283.